PHYSICAL REVIEW C VOLUME 15, NUMBER 4 APRIL 1977

28- and 34-MeV ^{6}Li and ^{7}Li elastic scattering on nuclei with $40 \leq A \leq 91$†

R. I. Cutler, M. J. Nadworny,* and K. W. Kemper
Physics Department, The Florida State University, Tallahassee, Florida 32306
(Received 23 November 1976)

^{6}Li and ^{7}Li elastic scattering were measured at 28 and 34 MeV on ^{40}Ca and ^{48}Ca to $\sigma/\sigma_R < 10^{-3}$. An anomalous back angle enhancement was seen for ^{6}Li + ^{40}Ca. No set of optical model parameters tried was able to fit the back angle ^{6}Li + ^{40}Ca data. Optical model parameters which exhibited a continuous Igo ambiguity but no discrete ambiguities were obtained for the above reactions and for other Li elastic scattering on ^{62}Ni, ^{63}Cu, ^{64}Zn, ^{68}Zn, ^{90}Zr, and ^{91}Zr. For a given value of the diffuseness, all parameter sets related by the Igo ambiguity gave completely identical fits to data. The value of the diffuseness which yielded acceptable fits was limited to a narrow range. It was found that the optical model parameters are extremely sensitive to the absolute normalization of the data. An empirical formula for the optical model parameters as a function of N and Z of the target nucleus was obtained for both ^{6}Li and ^{7}Li elastic scattering on these targets.

[NUCLEAR REACTIONS ^{40}Ca(^{6}Li, ^{6}Li), ^{40}Ca(^{7}Li, ^{7}Li), ^{48}Ca(^{6}Li, ^{6}Li), ^{48}Ca(^{7}Li, ^{7}Li); E=28 and 34 MeV; measured $\sigma(\theta)$, θ_{lab} =10–165°; deduced optical model parameters. Deduced systematic optical model parameters Li + ^{40}Ca, ^{48}Ca, ^{63}Cu, ^{64}Zn, ^{68}Zn, ^{90}Zr, ^{91}Zr.]

I. INTRODUCTION

The existence of high intensity Li beams has made it possible to study Li induced transfer reactions on moderately heavy targets, where the reaction cross sections are in the μb range. The present study was motivated by the need to have optical model parameters for use in direct reaction calculations as well as to search for systematics in Li elastic scattering. The present work contains data for ^{48}Ca + ^{6,7}Li and ^{40}Ca + ^{6,7}Li at 28 and 34 MeV measured to angles where $\sigma/\sigma_R < 10^{-3}$. These data are analyzed with the optical model. Previously measured data on ^{62}Ni,[1] ^{63}Cu,[1] ^{64}Zn,[2] ^{68}Zn,[2] ^{90}Zr,[3] and ^{91}Zr[3] were also included in the analysis to obtain optical model parameters as a function of the N and Z of the target.

II. EXPERIMENTAL PROCEDURE

The ^{6}Li and ^{7}Li beams used in this experiment were produced in an inverted sputter source[4] and injected at 90 kV into the Florida State University super FN tandem Van de Graaff accelerator. Data were taken on both ^{40}Ca and ^{48}Ca for ^{6}Li and ^{7}Li beam energies of 28 and 34 MeV. The ^{48}Ca targets were prepared by evaporating ^{48}Ca from isotopically enriched (96.8%) $CaCO_3$ with an electron beam onto 50 μg/cm^2 carbon backings. The ^{40}Ca targets were formed by evaporating natural calcium metal (96.9% ^{40}Ca) onto 15 μg/cm^2 C backings. A single ^{48}Ca target, 27 μg/cm^2 thick, was used, while ^{40}Ca target thicknesses ranged from 100 to 300 μg/cm^2. The rather expensive ^{48}Ca target was stored under an argon atmosphere between runs to prevent the formation of $Ca(OH)_2$, which would destroy the target. The ^{40}Ca targets were prepared immediately before each run in a special target barrel and transferred under vacuum to the scattering chamber.

Angular distributions were obtained from 10° to 165° (lab) in 2.5° steps for ^{40}Ca + Li, with 1.25° increments used for $\theta_{lab} \leq 40°$. The ^{48}Ca + Li measurements extended only to 75° lab due to the thinner target. Data were taken with a two- to four-detector array mounted in a 45-cm general purpose scattering chamber. For forward angle data ($\theta_{lab} \leq 40°$) and some back angle ^{6}Li data, single Si surface barrier detectors 150–300 μm thick were used. To eliminate interference from ^{12}C(^{6}Li, α) the counters were underbiased, reducing their effective depletion so as to only just stop the Li ions. Consequently, the α did not lose enough energy in these detectors to interfere with the Li elastic peak. This technique was not sufficient to eliminate the α contaminants for ^{6}Li measurements with $\theta_{lab} > 75°$ and for ^{7}Li with $\theta_{lab} > 40°$. Here, ΔE-E counter telescopes were used, each consisting of a 40-μm transmission type, (ΔE) totally depleted, Si surface barrier detector and a 300-μm Si surface barrier (E) detector. Two coincident signals from each telescope, suitably amplified, were stored pair-wise in an EMR 1630 computer via an analog-to-digital converter-CAMAC interface. The resultant data were displayed as a two-dimensional plot of ΔE vs E and gates were drawn with a light pen about the events in the region of interest. These events were then sorted into energy spectra.

The angular acceptance of each detector was

0.35° for $\theta_{lab} \leq 40°$ and 0.7° for $\theta_{lab} \geq 40°$. The energy resolution ranged from 130 to 180 keV full width at half maximum (FWHM). Beam current on target was limited to 250 nA Li^{+3} to avoid target evaporation; beam current and target conditions were monitored with a detector fixed at 25° lab. The count rate was low enough so dead time was less than 1% in all runs. Absolute normalization was done using 3.5-MeV proton scattering at $\theta_{lab} = 20°$, which was assumed to be Rutherford. To insure that the beam spots on target for the p and Li beams were identical, a 0.24-cm diameter beam collimator was mounted immediately in front of the target for the normalization runs in addition to the usual beam collimation used in the other runs.

Relative uncertainties due to the effects of statistics, peak fitting, and angle setting accuracy in the elastic cross sections are reflected by the error bars on the individual data points in the figures. If no error bars are present, the dot size equals or exceeds the relative error at that point. The absolute error in the normalization is 5%, consisting of uncertainties produced in the normalization data runs by beams integration (3%), peak fitting (3%), angle setting (2%), and statistics (1%). The elastic scattering angular distributions at 28 and 34 MeV for ^{6}Li and ^{7}Li from ^{40}Ca and ^{48}Ca are shown plotted as the ratio-to-Rutherford in Figs. 1–4. Because of the ability to produce thick ^{40}Ca targets, it was possible to measure data to much larger angles.

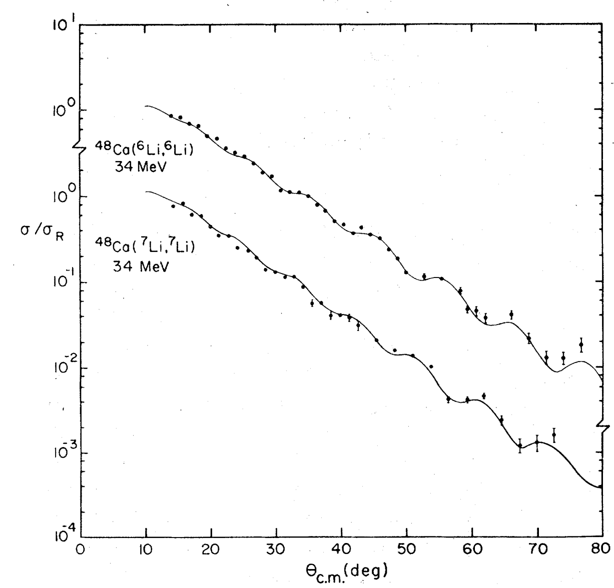

FIG. 1. Li + ^{48}Ca elastic scattering at 34 MeV. The optical model fits were obtained with the parameters in Table III. Identical fits were obtained for other Igo-related parameters.

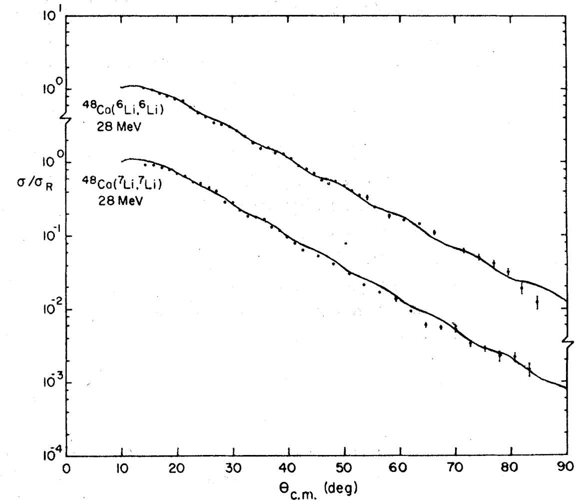

FIG. 2. Li + ^{48}Ca elastic scattering at 28 MeV. The optical model fits were obtained with the parameters in Table III. Identical fits were obtained for other Igo-related parameters.

III. OPTICAL MODEL ANALYSIS

A. ^{40}Ca and ^{48}Ca

The optical potential used in the analysis of the data was of the standard form

$$V(r) = \frac{-U}{1+\exp[(r-R_R)/a_R]} - \frac{iW}{1+\exp[(r-R_I)/a_I]} + V_C(r),$$

where

$$V_C(r) = \frac{Z_p Z_t e^2}{2R_C}[3-(r^2/R_C)^2], \quad r \leq R_C,$$
$$= \frac{Z_p Z_t e^2}{r}, \quad r > R_C,$$

with $R_C = 3.14 + 1.3 A_T^{1/3} = R_C(^6\text{Li}) + R_C(A_T)$ (Ref. 5) and $R_x = r_x(A_t^{1/3} + A_p^{1/3})$, with A_T (z_t) and A_p (Z_p) being the masses (charges) of the target and the projectile nuclei, respectively. The calculations were carried out with the computer code JIB.[6]

Initially, the real and imaginary diffusenesses a_R and a_I were set equal, as were the real and imaginary radius parameters (r_R and r_I). The four parameters U, W, r, and a were incremented in a four-dimensional χ^2 grid where U ranged from 20 to 300 MeV with $\Delta U = 10$ MeV, W ranged from 10 to 205 MeV with $\Delta W = 5$ MeV, r ranged from 0.7 to 1.7 fm with $\Delta r = 0.2$ fm, and a ranged from 0.4 to 1.0 fm with $\Delta a = 0.1$ fm. The value of $\chi^2 = \sum_{i=1}^{n}[(\sigma^i_{exp} - \sigma^i_{calc})/\Delta^i_{exp}]^2$ was calculated for

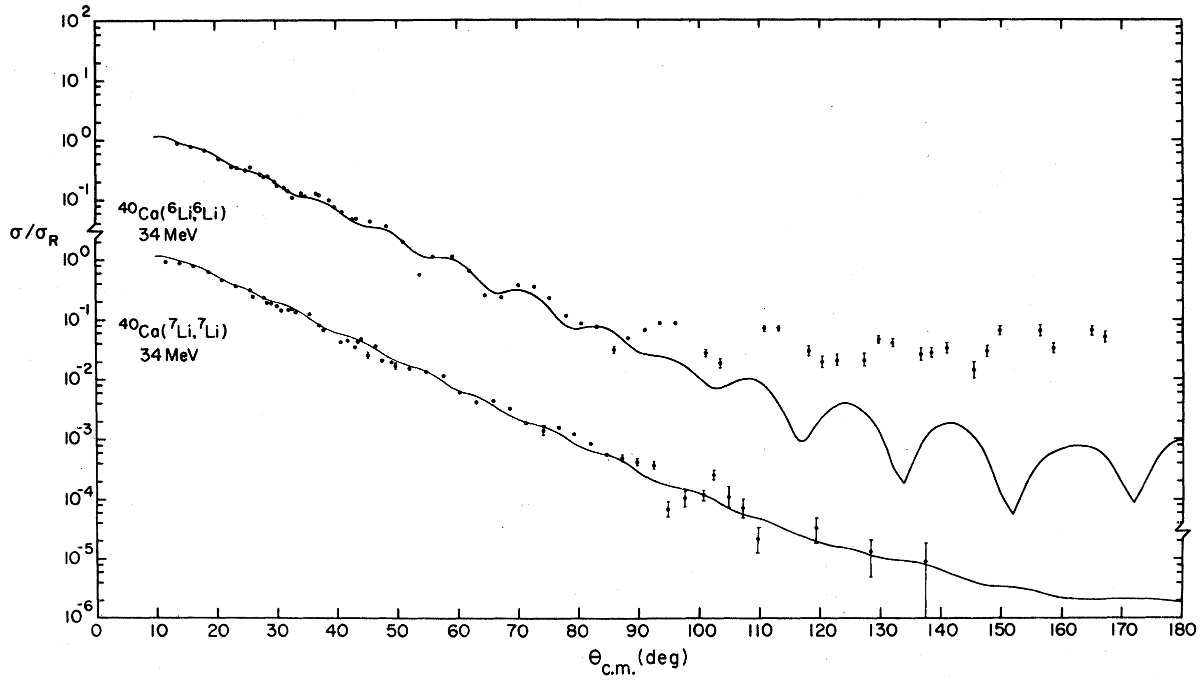

FIG. 3. Li + ^{40}Ca elastic scattering at 34 MeV. The optical model fits were obtained with the parameters in Table III. Identical fits were obtained for other Igo-related parameters.

each point in this grid using the ^{6}Li + ^{48}Ca at 34 MeV experimental data. These data were used because they were obtained first. There were several local χ^2 minima which occurred in this grid, and the value of the four parameters at these minima were searched upon to improve the fit of the optical model calculations to the data. The parameters r_R and r_I plus a_R and a_I were then

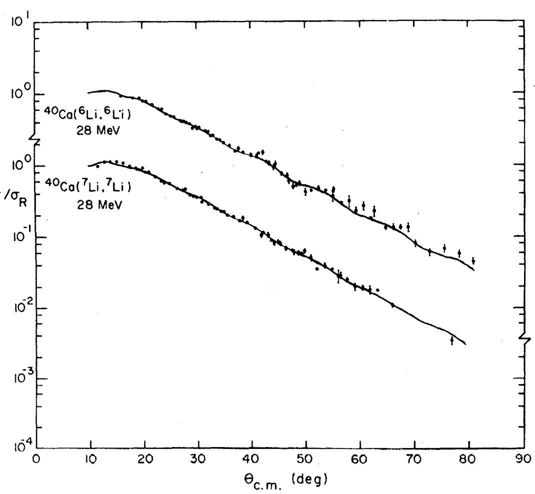

FIG. 4. Li + ^{40}Ca elastic scattering at 28 MeV. The optical model fits were obtained with the parameters in Table III. Identical fits were obtained for other Igo-related parameters.

uncoupled. Subsequent searching on all six parameters did not appreciably improve the fits. The parameters obtained in this manner were used as starting points for subsequent searching to fit the rest of the experimental data.

For a given value of r and a (i.e., fixed geometry), it was found that only one set of U and W fitted each of the experimental data sets; i.e., no discrete ambiguities were observed. However, when all four parameters are considered, a continuous Igo-type[7] ambiguity is seen to exist.

The value of a adopted in this study for the purpose of comparing different potential sets is 0.83 fm, the diffuseness which yielded the best fits to the 34 MeV ^{48}Ca + ^{6}Li data. It was found that only a very narrow range of diffusenesses, between 0.75 and 0.9 fm, would yield good fits to data. This is illustrated in Fig. 5, which shows a vs the χ^2 of the best fit obtained by varying U and W for ^{6}Li + ^{48}Ca at 34 MeV. For each experimental data set, there were several four-parameter sets which yielded identical theoretical angular distribution calculations and had similar Igo constants $I_R = Ue^{R_R/a_R}$ and $I_I = We^{R_I/a_I}$. Table I lists some parameter sets and their Igo constants which fit ^{48}Ca + ^{6}Li at 34 MeV.

In the past, it has been shown that certain Li optical model parameter sets describe reaction data better than other parameter sets,[8] even though all the parameter sets may fit the elastic scat-

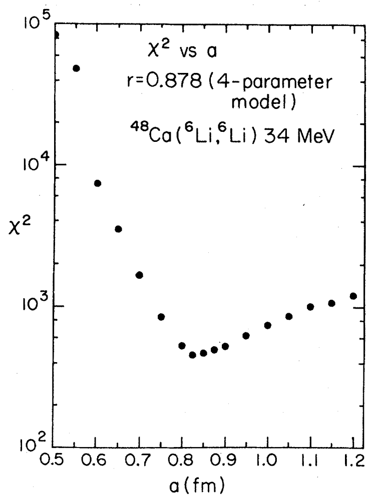

FIG. 5. χ^2 for four-parameter optical model fits as a function of diffuseness a with $r = 0.878$ fm for ^{6}Li + ^{48}Ca at 34 MeV. U and W were varied at each point to obtain the best fit.

tering data equally well. These sets typically are six-parameter fits with a large (>100 MeV) real well depth, and a small (~0.8 fm) real radius, a shallow imaginary well depth, and a large imaginary radius. One such parameter set was tried, and it gave fits to the elastic data which are identical to the four-parameter sets; it is also listed in Table I. The Igo constants for these types of parameter sets are similar to those of the four-parameter sets, suggesting that all of these parameter sets are related.

Identical sets of parameters fit ^{48}Ca + ^{6}Li and ^{48}Ca + ^{7}Li at 34 MeV, and other identical sets of parameters fit the 28 MeV ^{48}Ca + Li data. But for the ^{40}Ca data, this was not true. No consistent rule could be found for taking a given set of ^{40}Ca + ^{6}Li parameters and fitting other ^{40}Ca + Li data. It was not possible to fit the ^{40}Ca back angle data with any parameter variation. When the same angular range of data was selected for ^{40}Ca as for ^{48}Ca, it was still not possible to interchange the ^{6}Li and ^{7}Li optical parameters, as would be the case if the difficulties encountered in fitting the ^{40}Ca data arose solely because of the much larger angular range of data taken.

The back angle ^{6}Li + ^{40}Ca data appears to be anomalously high as is also seen in the α + ^{40}Ca reaction.[9] For ^{6}Li + ^{63}Cu, this enhanced back angle cross section was not observed. For this case, only an upper limit of $\sigma/\sigma_R < 10^{-5}$ at 165° could be established, whereas on ^{40}Ca, $\sigma/\sigma_R \sim 5\times10^{-4}$. Also, ^{6}Li + ^{40}Ca is enhanced by at least an order of magnitude relative to ^{7}Li + ^{40}Ca scattering, as can be seen in Fig. 3. At 165° only a limit of $<10^{-5}$ could be established for ^{7}Li + ^{40}Ca in the present work.

An attempt was made to fit the ^{6}Li + ^{40}Ca data using l-dependent potentials as used for α + ^{40}Ca (Ref. 9) and ^{16}O + ^{40}Ca (Ref. 10) elastic scattering, by multiplying the imaginary potential with $f(l) = \{1+\exp[(l-l_c)/\Delta l]\}^{-1}$. The inclusion of l dependence predicted a rise in the ratio-to-Rutherford cross section at far backward angles but the data in this case is essentially "flat" from 90°–165° lab. In addition, the justification for using an l-dependent potential for ^{6}Li scattering is not particularly good, since the large angular momentum mismatches for reaction channels with α and ^{16}O projectiles do not exist for ^{6}Li projectiles on ^{40}Ca.

Perey and Perey[11] have been able to describe the energy dependence of optical parameters for lighter projectiles as a linear function of the bombarding energy E, or at most a quadratic function of E only. Since the ^{48}Ca and ^{40}Ca data were taken at two energies, a fit to a linear function of E only was attempted. For ^{6}Li scattering, the energy dependence of the six-parameter set was similar for the ^{40}Ca and ^{48}Ca data, with U decreasing by 5.35 MeV and W decreasing by 0.91 MeV per MeV increase in bombarding energy. This dependence was found to yield parameters which matched the fit obtained by Bethge, Fou, and Zurmühle[12] for 20 MeV ^{6}Li on ^{40}Ca. For ^{7}Li

TABLE I. Sample optical model (OM) parameters for ^{48}Ca(^{6}Li,^{6}Li) at 34 MeV. The real and imaginary Igo constants (I_R, I_I) are also given. The nuclear potential radius is given by $R_x = r_x(A_T^{1/3} \pm A_P^{1/3})$, and the Coulomb radius by $R_C = 3.14 + 1.3A_T^{1/3}$ fm.

OM set	U (MeV)	r_R (fm)	a_R (fm)	W (MeV)	r_I (fm)	a_I (fm)	I_R (MeV)	I_I (MeV)
1	29.41	1.068	0.83	33.22	1.068	0.83	3.27×10^4	3.69×10^4
2	105.1	0.878	0.83	105.8	0.878	0.83	3.35×10^4	3.37×10^4
3	165.4	0.801	0.83	17.93	1.165	0.83	3.19×10^4	3.77×10^4
4	61.28	0.959	0.83	63.74	0.959	0.83	3.32×10^4	3.45×10^4
5	239.6	0.753	0.83	235.3	0.753	0.83	3.37×10^4	3.31×10^4
6	276.8	0.731	0.83	271.3	0.731	0.83	3.37×10^4	3.31×10^4

TABLE II. Sample optical model potentials for ^{62}Ni(^{7}Li, ^{7}Li) and ^{63}Cu(^{6}Li, ^{6}Li). The radius is given by $R_x = r_x (A_T^{1/3} + A_P^{1/3})$. I_R and I_I are the Igo constants. The Coulomb radius is $R_C = 3.14 + 1.3 A_T^{1/3}$ fm.

Reaction	OM set	Energy (MeV)	U (MeV)	r_R (fm)	a_R (fm)	W (MeV)	r_I (fm)	a_I (fm)	I_R (MeV)	I_I (MeV)
^{62}Ni(^{7}Li, ^{7}Li)	1	34	39.57	1.068	0.83	49.0	1.068	0.83	7.55×10^4	9.35×10^4
^{62}Ni(^{7}Li, ^{7}Li)	2	34	153.5	0.878	0.83	172.0	0.878	0.83	7.64×10^4	8.56×10^4
^{62}Ni(^{7}Li, ^{7}Li)	3	34	246.9	0.801	0.83	23.42	1.165	0.83	7.14×10^4	8.87×10^4
^{63}Cu(^{6}Li, ^{6}Li)	1	30.1	30.62	1.068	0.83	41.82	1.068	0.83	5.30×10^4	7.25×10^4
^{63}Cu(^{6}Li, ^{6}Li)	2	30.1	119.3	0.878	0.83	147.0	0.878	0.83	5.48×10^4	6.76×10^4
^{63}Cu(^{6}Li, ^{6}Li)	3	30.1	186.2	0.801	0.83	21.29	1.165	0.83	5.01×10^4	7.24×10^4

scattering, it was found that the ^{48}Ca and ^{40}Ca exhibited completely different energy dependence for both U and W. In the ^{7}Li + ^{48}Ca data, both U and W showed an energy dependence similar to the ^{6}Li + Ca data. However, the ^{7}Li + ^{40}Ca data showed an energy dependence for U and W of similar magnitude to the ^{6}Li data but of opposite sign, i.e., and increase in U and W with increasing bombarding energy. Based on our limited data, we can give no meaningful energy dependence for the ^{7}Li optical model parameters.

B. Analysis of Li + ^{62}Ni, ^{63}Cu, ^{64}Zn, ^{68}Zn, ^{90}Zr, and ^{91}Zr

Because of the possibility of having 10% differences in the absolute normalization of the previously measured Li scattering[1-3] to be included in the search for systematic optical potentials, the effect of absolute normalization on the parameters U and W was investigated. It was found that if the geometry were kept fixed, U and W would change by as much as 15% for a 3% difference in absolute normalization and by as much as 25% for a 7% difference in absolute normalization. Consequently, all previously measured Li elastic scattering data were renormalized. During the course of one run, Li scattering was performed at 34 MeV on all targets included in the global analysis. Then 4 MeV proton elastic scattering was performed. The proton scattering was assumed to be Rutherford so that the product of target thickness times solid angle was obtained. Since the solid angle was the same for each target, the proton scattering yielded a relative target thickness between the various targets of 3%, this error arising from the charge integration and detector angle setting errors. Because better than 10 000 counts were taken for the Li scattering, the relative error between different targets for the Li scattering was also 3%.

Using the optical model parameters found for Li + ^{48}Ca elastic scattering as initial values, U and W were searched upon to produce the best fit to the other lithium elastic scattering data sets which were taken previously at Florida State University.[1-3] Again, the continuous Igo ambiguity was observed as shown in Table II, which lists three differerent parameter sets and their constants for ^{7}Li + ^{62}Ni (34 MeV) and ^{6}Li + ^{63}Cu (30.1 MeV) elastic scattering. In both these cases and for ^{6}Li + ^{64}Zn (28 MeV), ^{6}Li + ^{90}Zr (34 MeV), ^{6}Li + ^{91}Zr (34 MeV), ^{7}Li + ^{64}Zn (34 MeV), ^{7}Li + ^{68}Zn (34 MeV), and ^{7}Li + ^{90}Zr (34 MeV), all three-parameter sets gave completely identical fits to data. Figure 6 shows the fits to the data for ^{6}Li + ^{63}Cu and ^{7}Li + ^{62}Ni.

One problem with the optical model is that paremeters which fit elastic scattering data may not describe reaction data very well, since elastic scattering only yields information about the tail region of the potential. From previous work,[8] it is known that potential sets similar to type number 3 give the best fits to reaction data. In Fig. 7 are shown the plots of three real potentials

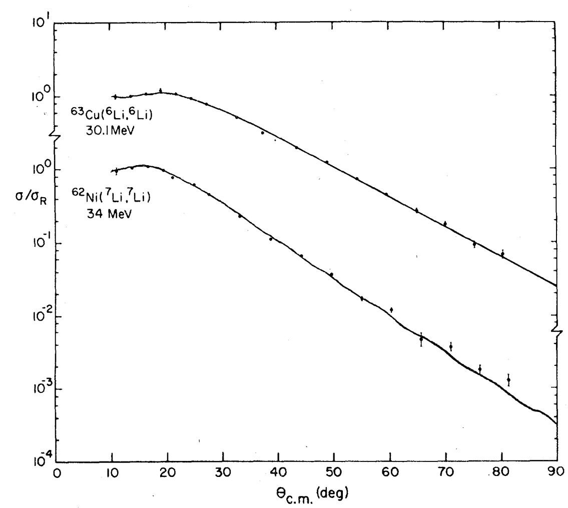

FIG. 6. ^{6}Li + ^{63}Cu at 30.1 MeV and ^{7}Li + ^{62}Ni at 34 MeV data and the optical model fits using parameters in Table III.

which gave completely identical fits to $^7Li + ^{62}Ni$ elastic scattering. It is seen that all three potentials are identical from 8 fm outward, but vary greatly inward of this point. The imaginary potentials behave similarly. The strong absorption radius in this case is at 10 fm. Table III lists six-parameter optical potentials for all the elastic scattering data included in the analysis.

To investigate the dependence of the elastic scattering on the N and Z of the target, it was assumed that U (or W) had the form $C_0 + C_1(N-Z)/A + C_2(Z/A^{1/3})$, which is a form used for lighter ions as reported in Perey and Perey.[11] The constants C_0, C_1, and C_2 were found by the method of least squares. For ^{6}Li scattering with geometry parameters of $r_R = 0.801$ fm, $r_R = 1.165$ fm, $R_C = (3.14 + 1.3)A^{1/3}$ fm, $a_R = a_I = 0.83$ fm, the potentials had the form U (MeV) $= -41.2 + 175(N-Z)/A + 31.4Z/A^{1/3} - 5.3(E_B - 34)$ and W (MeV) $= 4.16 + 12.2(N-Z)/A + 2.08Z/A^{1/3} - 0.91(E_B - 34)$, where E_B is the laboratory bombarding energy. For ^{7}Li at 34 MeV with the same geometry parameters U (MeV) $= -2.76 + 94.7(N-Z)/A + 28.8Z/A^{1/3}$ and W (MeV) $= 23.7 - 35.1(N-Z)/A + 4.37Z/A^{1/3}$. These potential sets gave excellent agreement with the fits obtained by Bethge[12] for ^{6}Li elastic scattering on ^{40}Ca at 20 MeV. They were less successful in fitting data outside the $A = 40-91$ mass region and did not agree with published optical model fits for Li + ^{26}Mg at 36 MeV,[8] ^{28}Si at 36 MeV,[8] or ^{118}Sn at 24 MeV.[13]

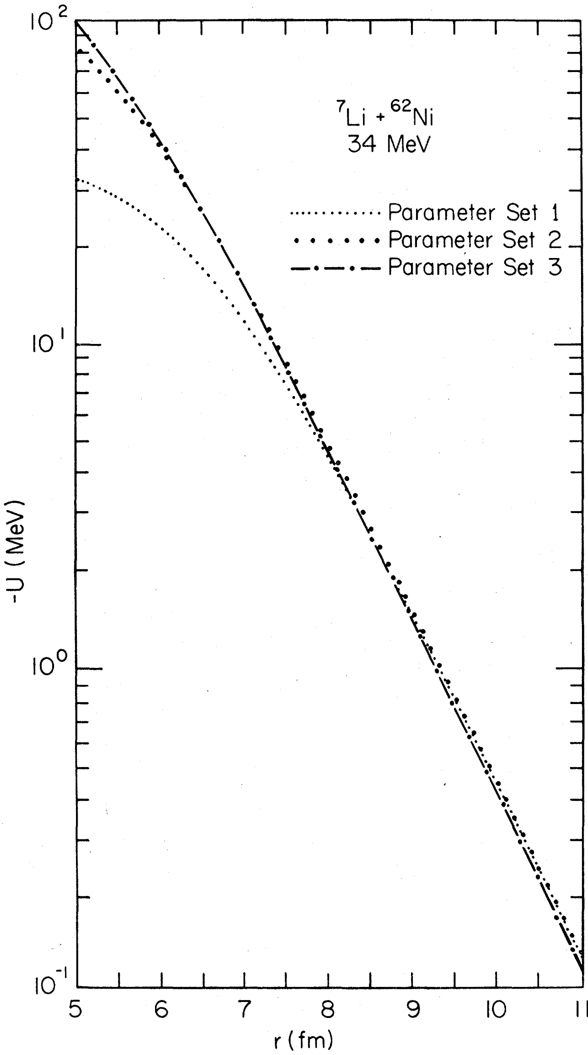

FIG. 7. Three real potentials ($-U$) for $^7Li + ^{62}Ni$ for parameter sets shown in Table II. Note that all three are the same from 8 fm outward.

IV. CONCLUSIONS

The purpose of this study was to investigate the systematics and ambiguities of optical model parameters for lithium elastic scattering on targets of $A \geq 40$. A large range of possible values for the parameters was investigated and no discrete ambiguities in the optical model parameters were observed. However, it was discovered that there existed many sets of parameters (both four and six member) related by a continuous Igo ambiguity which yielded completely identical elastic scattering cross sections and fitted the experimental data equally well. As the calculations proved to be identical, there was no method of determining which of the many parameter sets would fit reaction data as well as elastic scattering data using only the experimental elastic data. The ^{40}Ca data was even extended to far back angles to check if one data set would fit better in this region. The large angle $^{40}Ca + ^6Li$ data was found to be anomalously high and was not fitted by the standard optical model, or the optical model with l dependence.

The six-parameter set chosen in this work to fit all of the targets was one which has been previously shown to describe reaction data even though the elastic scattering did not favor this set over any other six-parameter or four-parameter set.

The optical model parameters themselves were found to be extremely sensitive to the absolute normalization of the data. This served to limit the accuracy of the parameters U and W (with r and a fixed) to 10% for a 3% uncertainty in the absolute normalization of the data. Within this accuracy, a semiempirical formula for ^{6}Li and ^{7}Li optical model parameters at 34 MeV was found

TABLE III. Six-parameter optical model parameters which also describe single nucleon transfer data. $a_R = a_I = 0.83$ fm, $r_R = 0.801$ fm, $r_I = 1.165$ fm, $R_x = r_x(A_T^{1/3} + A_P^{1/3})$, $R_C = 3.14 + 1.3A_T^{1/3}$ fm.

Reaction	Projectile energy (MeV)	U (MeV)	W (MeV)	I_R (MeV)	I_I (MeV)
$^{40}Ca(^6Li, ^6Li)$	28	190.9	23.75	2.99×10^4	3.70×10^4
$^{40}Ca(^6Li, ^6Li)$	34	152.2	18.62	2.39×10^4	2.90×10^4
$^{48}Ca(^6Li, ^6Li)$	28	190.9	23.75	3.68×10^4	4.99×10^4
$^{48}Ca(^6Li, ^6Li)$	34	165.4	17.93	3.19×10^4	3.77×10^4
$^{63}Cu(^6Li, ^6Li)$	30.1	186.2	21.29	5.01×10^4	7.24×10^4
$^{64}Zn(^6Li, ^6Li)$	28	253.7	23.11	6.97×10^4	8.12×10^4
$^{90}Zr(^6Li, ^6Li)$	34	257.8	24.75	1.13×10^5	1.71×10^5
$^{91}Zr(^6Li, ^6Li)$	34	272.7	26.20	1.21×10^5	1.85×10^5
$^{40}Ca(^7Li, ^7Li)$	28	142.3	17.99	2.44×10^4	3.20×10^4
$^{40}Ca(^7Li, ^7Li)$	34	156.6	24.03	2.69×10^4	4.28×10^4
$^{48}Ca(^7Li, ^7Li)$	28	190.9	23.75	4.04×10^4	5.71×10^4
$^{48}Ca(^7Li, ^7Li)$	34	165.4	17.93	3.50×10^4	4.31×10^4
$^{62}Ni(^7Li, ^7Li)$	34	246.9	23.42	7.14×10^4	8.87×10^4
$^{64}Zn(^7Li, ^7Li)$	34	220.4	20.40	6.64×10^4	8.20×10^4
$^{68}Zn(^7Li, ^7Li)$	34	206.7	18.10	6.74×10^4	8.16×10^4
$^{90}Zr(^7Li, ^7Li)$	34	255.4	20.66	1.22×10^5	1.63×10^5

for targets in the mass region $A = 40$ to 91. While projectile energy dependence of the parameters was not investigated in detail, it was found that for ^{6}Li scattering, both ^{40}Ca and ^{48}Ca optical model parameters U and W decreased with increasing projectile energy, but for ^{7}Li scattering the parameters U and W decreased for ^{48}Ca and increased for ^{40}Ca with increasing energy.

The authors wish to thank L. H. Harwood, L. J. House, and R. J. Puigh, III, for their assistance in obtaining the data used in this report.

† Work supported in part by National Science Foundation Grants Nos. NSF-PHY-7503767-A01, NSF-GU-2612, and NSF-GJ-367.

* Present address: Department of Mathematics, Cairo High School, Cairo, Georgia.

[1]R. L. White and K. W. Kemper, Phys. Rev. C 10, 1372 (1974).
[2]G. M. Hudson, Ph.D. thesis, Florida State University, 1976 (unpublished).
[3]R. J. Puigh, Ph.D. thesis, Florida State University, 1976 (unpublished).
[4]K. R. Chapman, Nucl. Instrum. Methods 124, 299 (1975).
[5]H. R. Collard, L. R. B. Elton, and R. Hofstadter, in *Nuclear Radii*, edited by H. Schopper (Springer-Verlag, Berlin, 1967).
[6]F. G. Perey, Phys. Rev. 131, 745 (1963); A. W. Obst, Florida State University Technical Report JIB, 1973 (unpublished).
[7]G. Igo, Phys. Rev. Lett. 1, 2 (1958); Phys. Rev. 115, 1665 (1959).
[8]G. M. Hudson, K. W. Kemper, G. E. Moore, and M. E. Williams, Phys. Rev. C 12, 474 (1975); P. Schumacher, N. Ueta, H. H. Duhm, K.-I. Kubo, and W. J. Klages, Nucl. Phys. A212, 573 (1973).
[9]A. E. Bisson, K. A. Eberhard, and R. H. Davis, Phys. Rev. C 1, 539 (1970).
[10]J. S. Eck, R. A. LaSalle, and D. Robson, Phys. Rev. 186, 1132 (1969).
[11]C. M. Perey and F. G. Perey, Atom. Data Nucl. Data Tables 17, 1–107 (1969).
[12]K. Bethge, C. M. Fou, and R. W. Zurmühle, Nucl. Phys. A123, 521 (1969).
[13]K. O. Pfeiffer, E. Speth, and K. Bethge, Nucl. Phys. A206, 545 (1973).